



## AN OPEN SOURCE SOFTWARE FOR PULSATION ANALYSIS OF PIPELINE SYSTEMS

**Jacson G. Vargas**

LVA – Acoustics and Vibration Lab  
UFSC – Federal University of Santa Catarina  
Florianópolis, Brazil  
jgvargasemc@gmail.com

**Olavo M. Silva**

MOPT – Multidisciplinary Optimization Group  
UFSC – Federal University of Santa Catarina  
Florianópolis, Brazil  
olavo@lva.ufsc.br

### ABSTRACT

Acoustically Induced Vibration (AIV) can be a cause of failure in gas pipeline systems pressurized by reciprocating compressors. *OpenPulse* is an open-source software written in Python for numerical modelling of low-frequency AIV. It allows to import the geometry of the pipe system, insert materials properties, set sections, and import pressure/acceleration/force loads (from measurements or theory). The computational procedure performs a time-harmonic acoustic response analysis of the respective 1D acoustic domain using the Finite Element Transfer Matrix Method (FETM). The resulting pressure field is applied as a distributed load over the respective structural piping system, modeled with the Timoshenko beam theory and the Finite Element Method (FEM). This strategy is presented using a simple application with a particular set of boundary conditions, where nodal pressure and displacement frequency plots are presented at some points of the system.

**Keywords:** Pulsation, pipeline systems, FEM, FETM

### 1. INTRODUCTION

In oil refinery plants, large reciprocating compressors represent an important source of excitation for gas pipeline systems. This kind of excitation is known as Acoustically Induced Vibration (AIV) and is an important vibration mechanism in pipeline systems, which responds to both unsteady and pulsating flow fields [1].

Approximate acoustic models are often used to calculate frequency-domain solutions for AIV [2]. The most common methods are: the Method of Characteristics (MOC) [3]; the Finite Element Method (FEM) [4]; the Matrix

Condensation Method (MCM) [5]; the Transfer Matrix Method (TMM) ([1, 5]); and, finally, hybrid techniques that consists in combinations between the aforementioned methods like the MOC-FEM [3], the Finite Element Transfer Method (FETM) [5] sometimes called as the Stiffness Matrix Method (SMM), as well as others. On the other hand, the structural response of the pipes is often obtained by FEM.

The objective of this work is to predict the acoustic and the structural harmonic responses of pipeline systems subjected to internal “low-frequency” distributed loads (internal acoustic pulsation in frequencies equivalent to the first harmonics of typical compressors pulsation’s spectra). It is assumed that the pipes are composed of linear elastic isotropic materials, with length much larger than the diameter and deflections sufficiently small compared to the pipe thickness. The target is to analyze the global structural behavior of the pipeline system, which here is considered as a system of beams. Also, it is considered a “weak” coupling between structural and acoustic fields based on the resultant structural stresses over the pipe wall (obtained analytically from pipe section dimensions and internal pressure), which is converted in axial structural forces. One can also adopt the methodology proposed in this work to predict airborne noise-induced vibrations or for evaluating possible risks due to airborne noise.

It is assumed that there is an acoustic field through a non-dissipative ideal gas inside each pipe/duct, and the structural vibration response of the pipe can be represented by the Timoshenko beam theory, for a defined domain and a set of boundary conditions. The problem is modeled by a combination of FETM (for acoustic field) and FEM (for structural field) considering reciprocating compressor pulsation as the main source of excitation under time-

harmonic plane wave assumption. Here, the FETM, which can be numerically implemented in the same way as FEM, enables simulating complex geometries and facilitates the weak coupling procedure.

An open source code called *OpenPulse* [6] was developed in Python to solve the AIV problem and, also, to solve separately the acoustic or the structural problem, when necessary. In this article, it is presented the main physical and numerical concepts that are used to develop *OpenPulse*, and the effectiveness of the adopted strategy is demonstrated using a simplified example application. The related engineering project is at an early stage, and preliminary results are demonstrated without experimental validation. This work is an update of the article presented at ISMA2020 (Leuven - Belgium) [2] and similar with that presented at FIA 2022 (Florianopolis - Brazil) [7].

## 2. MODELLING THE ACOUSTIC DOMAIN

TMM method is particularly efficient to deal with plane acoustical waves in tubular circuits, because of the following aspects of the formulation [8]: (i) two scalar fields  $p$  and  $q$  are sufficient to describe the waves; (ii) it uses exact analytical wave solutions for low order modes propagation (plane waves); (iii) only a few types of transfer matrices are necessary for assembling discretized tubular models; (iv) certain implementations and changes in boundary conditions (i.e., nodal impedances, position and kind of nodal sources) and extension to dissipative problems can be done maintaining the element formulation. Consider a hard-walled straight uniform duct element as shown in Fig. 1. Gas properties like mean density  $\rho_f$  and speed of sound  $c_f$  are assumed to be uniform inside the tube. Volume velocity and pressure at the inlet of the element are denoted as  $q_1$  and  $p_1$ , while  $q_2$  and  $p_2$  denote the corresponding quantities at the outlet.  $Z$  represents the acoustical impedance of the tube element. The objective is to find a matrix equation that expresses the volume velocity  $q(x, k)$  and the pressure  $p(x, k)$  at any point  $x$  inside the tube element at the wavenumber  $k = \omega/c_f$ , in terms of their values at the inlet. The tube element can be represented as a linear system with two inputs and two outputs as follows:

$$\begin{bmatrix} p_2 \\ q_2 \end{bmatrix} = \mathbf{T}^e \begin{bmatrix} p_1 \\ q_1 \end{bmatrix}, \quad (1)$$

where  $\mathbf{T}^e$  is the 2x2 transfer matrix for the uniform tube element. By definition, the domain of fluid in a tube is characterized by one dimension,  $x$ , which is much larger

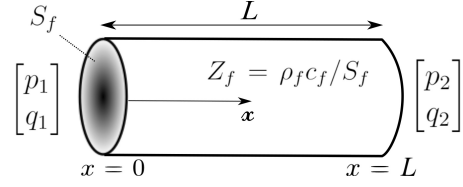


**Figure 1.** Uniform tube element (adapted from [8]).

than the others. For large wavelengths, we can assume constant pressure in the whole tube cross-section with radius  $r$  (low frequency). For this simple case, the homogeneous and non-dissipative wave equation is

$$p_{(xx)} - \frac{1}{c_f^2} p_{(tt)} = 0. \quad (2)$$

Then, the 1D solution can be written in terms of traveling waves and the components of the transfer matrix  $\mathbf{T}^e$  are obtained. Thus, Eq. 1 can be written as

$$\begin{bmatrix} p_2 \\ q_2 \end{bmatrix} = \begin{bmatrix} \cos(kx) & -iZ_f \sin(kx) \\ -\frac{i}{Z_f} \sin(kx) & \cos(kx) \end{bmatrix} \begin{bmatrix} p_1 \\ q_1 \end{bmatrix}, \quad (3)$$

where  $Z_f = \rho_f c_f / S_f$  is the acoustic fluid impedance. Observe that  $\mathbf{T}^e$  is not symmetric because of the choice made in the definition of the input and output vectors, which mix kinematics and stress variables (mixed formulation) [8]. To relate the TMM with a FEM-like matrix form, a few algebraic operations need to be done to rearrange the variables of the mixed formulation into one not mixed, which is more suitable with the FEM matrices. In structural mechanics, this method is known as FETM [9]. So, the TMM system of Eq. 3 can be adapted into the form (for a given duct element  $e$ )

$$\mathbf{K}_A^e \mathbf{p}^e = \mathbf{q}^e, \quad (4)$$

where  $\mathbf{q}^e = [q_1, q_2]'$  and  $\mathbf{p}^e = [p_1, p_2]'$  are the nodal volume velocities and the nodal pressures, respectively.  $\mathbf{K}_A^e$  is the elementary matrix for a straight tube, which is presented in the expanded form of Eq. 4:

$$\begin{bmatrix} -i \cot(kx) / Z_f & i / Z_f \sin(kx) \\ i / Z_f \sin(kx) & -i \cot(kx) / Z_f \end{bmatrix} \begin{bmatrix} p_1 \\ p_2 \end{bmatrix} = \begin{bmatrix} q_1 \\ q_2 \end{bmatrix}. \quad (5)$$

The matrix  $\mathbf{K}_A^e$  is known as the element Mobility Matrix [10]. In order to obtain the global acoustic behavior of the system, the elementary matrices  $\mathbf{K}_A^e$  are assembled

respecting the connectivity of each pipe element. The global mobility matrix  $\mathbf{K}_A$  is obtained doing the same procedure as adopted in FEM (see, e.g., [11]). In this work, each 1D acoustic element has two nodes and each node has 1 degree-of-freedom (DOF) (pressure). Also, the elements can have arbitrary length and cross-sectional area without harming the continuity of the field variables  $p$  and  $q$ . Thus, for a given excitation frequency  $\omega$ , the global acoustic system is

$$\mathbf{K}_A \mathbf{p} = \mathbf{q}, \quad (6)$$

where  $\mathbf{K}_A$  is the global Mobility Matrix,  $\mathbf{p}$  are the nodal pressures and  $\mathbf{q}$  are the nodal volume velocities for the whole system.

In the system presented in Eq. 6, the global pressure vector  $\mathbf{p}$  is presented as an unknown variable and must be found. Before solving the system, it is necessary to consider the application of BC's, which can be classified as: i) nodal volume velocity,  $q_i$ ; ii) nodal pressure,  $p_i$ ; iii) nodal acoustic impedance,  $Z_i$ , or element acoustic impedance,  $Z_{ij}$ . Some components like valves, cylinders, filters, etc. can be considered by their equivalent acoustic impedances. These BC's can vary with the frequency. For example, one can consider to apply a table of pressure obtained from an experiment or to apply a table of acoustic impedance that represents a valve, etc. Besides that, *OpenPulse* brings a simplified analytical model of a reciprocating compressor, enabling the obtaining of the resultant volume velocity for different construction/operation parameters. More details on the implementation of BC's used in this work can be found in [6].

Some features also implemented in *OpenPulse* that are detailed in [6]: capability of considering a mean flow velocity; adjustment of effective element lengths depending on the transition of pipe diameters (e.g., in expansion chambers and side branches); materials properties can be associated to different regions, making it possible to change gas properties according to the operational characteristics of each region of the domain (temperature, mean pressure, etc); addition of dissipation through inserting a complex wave number  $\bar{k}$ , if needed.

### 3. MODELLING THE STRUCTURAL DOMAIN

Structural FEM models based on beam theory are well consolidated for predicting global vibrations of pipe systems. The classical Timoshenko beam theory requires only  $C^0$ -continuity, enabling the use of finite element shape functions that are easily constructed. It is initially assumed that the  $\{x_1^e, x_2^e, x_3^e\}$ -axes are locally defined at the

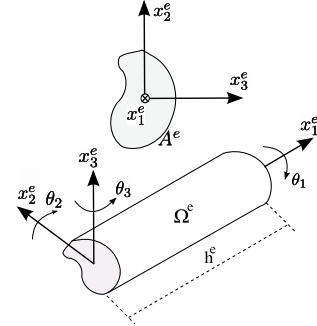


Figure 2. 3D beam local coordinates.

centroid of the beam segment cross-section and are principal axes [11], as can be seen in Fig. 2. A more detailed assumption is considered in *OpenPulse* [6], but the present one is sufficient to explain the structural modelling without losing of physical meaning.

The tridimensional displacements of a point  $(x_1, x_2, x_3)$  that belongs to a cross-sectional area  $A^e$  placed in  $x_1$  are given by [11, 12]:

$$u_1(x_1, x_2, x_3, t) = w_1(x_1, t) - x_2 \theta_3(x_1, t) + x_3 \theta_2(x_1, t), \quad (7)$$

$$u_2(x_1, x_2, x_3, t) = w_2(x_1, t) - x_3 \theta_1(x_1, t), \quad (8)$$

$$u_3(x_1, x_2, x_3, t) = w_3(x_1, t) + x_2 \theta_1(x_1, t). \quad (9)$$

Consequently, the movement of a given point  $(x_1, x_2, x_3)$  in the element domain  $\Omega^e$  is described by  $u(x_1, x_2, x_3, t) = [u_1, u_2, u_3]$ .

The translation components  $w_i$  of the neutral line and the rotation angles  $\theta_i$  of the sectional area are illustrated in Fig. 3. These kinematic constraints do not include warping (the plane sections remain plane). Besides that, it is considered that  $w_1, w_2$  and  $w_3$  are small when compared to  $h^e$ , and  $\sin \theta_i \approx \tan \theta_i \approx \theta_i$ . Assuming the local condition of mechanical equilibrium in a continuum medium  $\Omega$ , and considering the virtual displacement field  $\bar{u}$  (a kinematic admissible field), the variational equation can be written as [11]

$$\int_{\Omega} \bar{u}_{(ij)} \sigma_{ij} d\Omega - \int_{\Omega} \bar{u}_i F_i d\Omega - \int_{\Gamma_k} \bar{u}_i k_i d\Gamma + \int_{\Omega} \bar{u}_i \rho \ddot{u}_i d\Omega = 0, \quad (10)$$

where  $\Gamma_k$  is the boundary of  $\Omega$  where Neumann boundary conditions  $k_i$  are applied (at normal direction  $n$ ). The entity  $F$  represents the body forces acting on  $\Omega$  and  $\rho$  is the

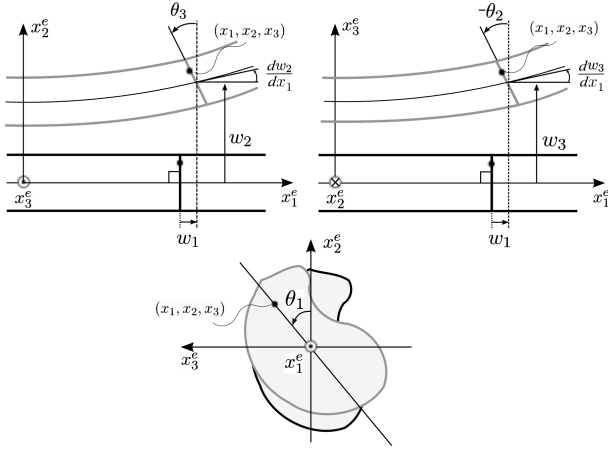


**Figure 3.** Deformation components in Timoshenko beam theory.

density of the material. The sub-indexes inside parenthesis indicate derivatives.

Considering  $dA = dx_2 dx_3$ , the domain can be represented by elements as follows:

$$\int_{\Omega} d\Omega = \sum_{e=1}^{nel} \int_{\Omega_e} d\Omega = \sum_{e=1}^{nel} \int_0^{h_e} \int_{A^e} dA dx_1. \quad (11)$$

Assuming  $\Gamma_k = \{\emptyset\}$  due to the “line shape” of the simplified structure [11], it is applied the hypothesis that all distributed external loads (force/length or moment/length) can be considered in the body force vector  $F$ . By this way, Eq. 10 can be rewritten using a matricial form, emphasizing that the integration is performed over the element length:

$$0 = \sum_{e=1}^{nel} \left\{ \int_0^{h_e} \left[ \bar{\gamma}^T \mathbf{D}^s \gamma + \bar{\kappa}^T \mathbf{D}^b \kappa + \bar{\varepsilon} (EA^e) \varepsilon + \bar{\Psi} (\mu J^e) \Psi \right] dx_1^e - \int_0^{h_e} \left[ \bar{w}^T F + \bar{\theta}^T C \right] dx_1^e + \int_0^{h_e} \left[ \bar{w}^T \mathbf{G}^{tr} \dot{w} + \bar{\theta}^T \mathbf{G}^r \dot{\theta} \right] dx_1^e \right\}, \quad (12)$$

where [11]

$$w = \begin{bmatrix} w_1 \\ w_2 \\ w_3 \end{bmatrix}, \theta = \begin{bmatrix} \theta_1 \\ \theta_2 \\ \theta_3 \end{bmatrix}, \quad (13)$$

$$\gamma = \begin{bmatrix} \gamma_2 \\ \gamma_3 \end{bmatrix}, \kappa = \begin{bmatrix} \kappa_2 \\ \kappa_3 \end{bmatrix}, \quad (14)$$

$$\mathbf{D}^s = \begin{bmatrix} \mu A_s^e & 0 \\ 0 & \mu A_s^e \end{bmatrix}, \mathbf{D}^b = \begin{bmatrix} EI_2^e & 0 \\ 0 & EI_3^e \end{bmatrix}, \quad (15)$$

$$\mathbf{G}^{tr} = \begin{bmatrix} \rho A^e & 0 & 0 \\ 0 & \rho A^e & 0 \\ 0 & 0 & \rho A^e \end{bmatrix}, \quad (16)$$

$$\mathbf{G}^r = \begin{bmatrix} \rho J^e & 0 & 0 \\ 0 & \rho I_2^e & 0 \\ 0 & 0 & \rho I_3^e \end{bmatrix}, \quad (17)$$

and:  $\Psi = \theta'_3$ ;  $\kappa_\beta = \theta'_\beta$  is called “curvature”;  $\varepsilon = w'_1$ ;  $\gamma_2 = w'_2 - \theta_3$ ;  $\gamma_3 = w'_3 + \theta_2$ ;  $F_i = \{F_i^e\}$  and  $C_i = \{C_i^e\}$  are the element applied external forces and couples, respectively, per unity length, for  $1 \leq e \leq nel$ . In order to simplify the presentation of the main hypotheses, the assumption that  $\{x_1^e, x_2^e, x_3^e\}$ -axes are locally defined at the centroid of the beam segment cross-section (and that they are principal axes) decouples bending from axial strain, in addition to decoupling torsional from transversal strain. In *Open-Pulse*, a more real assumption is considered (see [6]).

In the above equations,  $J^e, I_2^e$  and  $I_3^e$  are the area moments of inertia and  $A_s^e$  is the effective shear area considering a representative shear correction factor.

Considering  $\mathbf{N}$  the matrix of shape functions, and  $\mathbf{B}^a, \mathbf{B}^b, \mathbf{B}^s$  and  $\mathbf{B}^s$  the matrices of shape functions derivatives depending on the strain evaluated in Eq. 12, the element stiffness matrix  $\mathbf{K}^e$  is obtained as [11]

$$\mathbf{K}^e = \mathbf{K}_b^e + \mathbf{K}_s^e + \mathbf{K}_a^e + \mathbf{K}_t^e, \quad (18)$$

where

$$\mathbf{K}_b^e = \int_0^{h_e} \mathbf{B}^{bT} \mathbf{D}^b \mathbf{B}^b dx_1^e \text{ (bending stiffness)}, \quad (19)$$

$$\mathbf{K}_s^e = \int_0^{h_e} \mathbf{B}^{sT} \mathbf{D}^s \mathbf{B}^s dx_1^e \text{ (shear stiffness)}, \quad (20)$$

$$\mathbf{K}_a^e = \int_0^{h_e} \mathbf{B}^{aT} (EA) \mathbf{B}^a dx_1^e \text{ (axial stiffness),} \quad (21)$$

$$\mathbf{K}_t^e = \int_0^{h_e} \mathbf{B}^{tT} (\mu J) \mathbf{B}^t dx_1^e \text{ (torsional stiffness).} \quad (22)$$

The element mass matrix  $\mathbf{M}^e$  is obtained as

$$\mathbf{M}^e = \mathbf{M}_{tr}^e + \mathbf{M}_r^e, \quad (23)$$

where

$$\mathbf{M}_{tr}^e = \int_0^{h_e} \mathbf{N}^{trT} \mathbf{G}^{tr} \mathbf{N}^{tr} dx_1^e \text{ (translational mass),} \quad (24)$$

$$\mathbf{M}_r^e = \int_0^{h_e} \mathbf{N}^rT \mathbf{G}^r \mathbf{N}^r dx_1^e \text{ (rotational mass).} \quad (25)$$

Considering  $\mathbf{F}_{intg} = [F_1, F_2, F_3, C_1, C_2, C_3]'$ , the element force vector is obtained as follows:

$$\mathbf{f}^e = \int_0^{h_e} \mathbf{N}^T \mathbf{F}_{intg} dx_1^e. \quad (26)$$

To obtain the global structural behavior of the system, the elementary entities  $\mathbf{K}_e$ ,  $\mathbf{M}_e$  and  $\mathbf{f}_e$  are assembled, after local to global coordinate system transformation, respecting the connectivity of each beam element. The elements can have arbitrary length and cross-sectional area without harming the continuity of the field variables. After the assembling procedure, the global structural system is (considering damping)

$$(\mathbf{K} + j\omega\mathbf{C} - \omega^2\mathbf{M})\mathbf{d}(\omega) = \mathbf{f}(\omega). \quad (27)$$

In the global system presented in Eq. 27, the global vector  $\mathbf{d}$  is presented as an unknown variable and must be found. Before solving the system, it is necessary to consider the applications of the BC's, which can be classified as: i) nodal forces and/or moments,  $f_i$ ; nodal displacements and/rotations,  $d_i$ ; nodal lumped parameters: mass, spring and dampers. These BC's can vary with the frequency. For example, one can consider to apply a table of accelerations obtained from an experiment, or to apply a table of spring stiffness that represents supports, etc. More details on the implementation of BC's used in this work can be found in [6].

Some features also implemented in *OpenPulse* that are detailed in [6]: possibility of applying an offset between local coordinates and the beam's neutral axis; calculation of section properties and shear correction factor through a FE mesh of each section; different materials can be associated to different regions, making it possible to change pipe

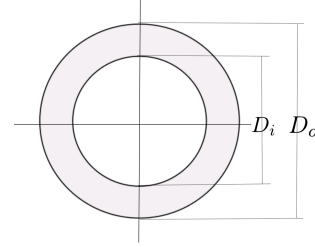


Figure 4. Section of the pipe element.

properties according to the operational/structural characteristics of each part of the domain; addition of distributed mass for representing insulation material, if relevant.

#### 4. ACOUSTIC-STRUCTURE ONE-WAY COUPLING

In the previous sections, the acoustic behavior of the fluid being transported throughout pipes and the structural behavior of pipeline systems were described independently. However, the objective of this work is to predict the dynamic response of structural systems subjected to harmonic acoustic loads.

In this work, we consider the structural pipe element as a beam with a hollow section, as can be seen in Fig. 4. The acoustic pipe element is configured in such a manner that the FETM mesh is the same as that used for FEM structural analysis. Additionally, the acoustic pipe element diameter equals to the internal structural diameter  $D_i$  considered in the respective beam element. In this work it is assumed a "weak" coupling (one-way coupling) based on the following hypotheses: the fluid is a gas; the viscosity of the fluid is negligible; the acoustic plane wave propagates in axial direction (1-D acoustics); the pipe is thin-walled and linearly elastic; the radial inertia of the pipe wall is neglected if considering low frequencies ( $ka \ll 1$ ); the acoustic wave speed  $c_f$  in the gas is affected by the mechanical compliance of the pipe wall and is given by:

$$c_f = \left( \frac{\rho_f}{K_f} \left( 1 + \frac{D_i K_f}{Et} \right) \right)^{-1/2} \quad (28)$$

where  $\rho_f$  is the fluid mass density,  $K_f$  is the fluid bulk modulus,  $E$  is the Young's modulus of pipe material,  $D_i$  is the internal diameter and  $t$  is the pipe wall thickness; resultant normal and shear stresses in the structure are derived



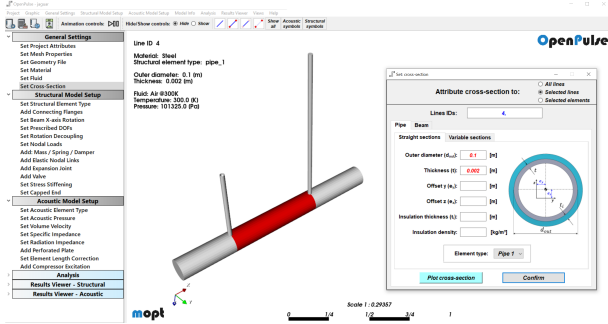


**Figure 5.** Main window of *OpenPulse*. Entry of properties and section parameters.

from the internal fluid pressure under the assumptions: i) plane stress conditions in the wall; ii) cross sections remain plane to the neutral axis.

Considering the assumptions listed above, the load equivalent to the stress field induced by the pressure effect is applied on each element as an external axial load, considering harmonic pulsation/vibration with an excitation frequency  $\omega$ .

The axial stress is resultant from the difference between internal and external pressure, and is given by [13]:

$$\sigma_1(\omega) = \frac{p_i(\omega)D_i^2 - p_o D_o^2}{D_o^2 - D_i^2}, \quad (29)$$

where  $p_i(\omega)$  is the internal pressure, obtained from the acoustic problem defined in Eq. 6 considering Eq. 28;  $D_i$  is the internal diameter;  $D_o$  is the external diameter; and  $p_o$  is the external pressure, considered constant in this work. The radial stress can be obtained using the Lamé stress distribution [13], using the internal and external pressures as a boundary condition:

$$\sigma_r(r, \omega) = \frac{p_i(\omega)D_i^2 - p_o D_o^2}{D_o^2 - D_i^2} - \frac{D_i^2 D_o^2 (p_i(\omega) - p_o)}{4r^2 (D_o^2 - D_i^2)}. \quad (30)$$

And the hoop (circumferential) stress is obtained using the same stress distribution considered in the radial case, resulting in:

$$\sigma_c(r, \omega) = \frac{p_i(\omega)D_i^2 - p_o D_o^2}{D_o^2 - D_i^2} + \frac{D_i^2 D_o^2 (p_i(\omega) - p_o)}{4r^2 (D_o^2 - D_i^2)}. \quad (31)$$

Consequently, the axial equivalent forces acting at both ends of each element can be found, and the additional element load vector  $\mathbf{f}_p^e$ , which must be added to Eq. 26, is

given by:

$$\mathbf{f}_p^e = \left[ -F_p, 0, 0, 0, 0, 0, F_p, 0, 0, 0, 0, 0 \right]', \quad (32)$$

where

$$F_p = A_e E \left[ \frac{1}{E} (\sigma_1 - \nu(\sigma_r + \sigma_c)) \right]. \quad (33)$$

After this procedure, the new element load vectors  $\mathbf{f}_p^e$  can be assembled and added to the global vector  $\mathbf{f}$ , which allows the calculation of the displacements vector  $\mathbf{d}$  through Eq. 27. The axial stress  $\sigma_1$  is considered only in the “capped end” condition [6].

The mass of the gas is considered distributed throughout the length of the structural elements. Thus, the matrix  $\mathbf{G}^{tr}$  in Eq. 16 is modified as follows

$$\mathbf{G}^{tr'} = \mathbf{G}^{tr} + \begin{bmatrix} \rho_f A_i & 0 & 0 \\ 0 & \rho_f A_i & 0 \\ 0 & 0 & \rho_f A_i \end{bmatrix}, \quad (34)$$

where  $A_i$  is the internal area of the pipe, calculated with  $D_i$ .

## 5. IMPLEMENTATION AND USER INTERFACE USING PYTHON

*OpenPulse* is an open-source software written in Python 3.7.7, with the requirement of installing the libraries numpy, scipy, vtk, PyQt5, Gmsh, h5py and matplotlib. A friendly interface (see Fig. 5) allows the user to import the geometry of the pipe system (lines in IGES format), insert materials properties, set sections, and import pressure/acceleration/force loads (from measurements or theory), as can be seen in Fig. 6. After defining the FEM mesh for the model, the user can plot the piping system geometry, see the FE mesh, and run the desired simulations after a proper setup. It is possible to plot deformed shapes, frequency plots of acoustical and structural responses, stress fields, and local stresses of desired sections. The code and a more detailed description of the implementation can be found in [6].

## 6. SIMPLIFIED EXAMPLE OF APPLICATION

In this section, the simplified piping system presented in Fig. 7a is analyzed. The maximum pipe length in the model is 2.25 m. The element size for acoustic and structural analyses is 0.01 m (the same mesh is used in both analyses). The external and internal diameters are  $D_o = 0.05$  m

and  $D_i = 0.034$  m. An expansion chamber is considered with  $D_o = 0.2$  m and  $D_i = 0.184$  m. The structure is modelled considering steel pipes with  $E = 210$  GPa,  $\nu = 0.3$  and  $\rho = 7860$  kg/m<sup>3</sup>. The gas being transported is hydrogen with  $\rho_f = 0.087$  kg/m<sup>3</sup> and  $c_f = 1321.1$  m/s. In this simple example, no dissipation or damping is considered. A general compressor is set to have the volumetric flow depicted in Figure 7b.

An acoustic impedance is applied at the end of the piping system to simulate an infinite tube. For the structure, it is considered a fixation of some translational movements (rotations free) in the nodes marked in green in Figure 7a. Remembering that it is possible to set other boundary conditions for structural analysis as forces, vibrations, springs, etc. According to the parameters of the compressor considered, the harmonic analysis is set to run from 0 to 200 Hz, with increments of 2 Hz.

The acoustic and structural responses of the piping system are presented in Fig. 8 for an excitation frequency of 12 Hz (fundamental frequency in the spectrum of the excitation pressure). The frequency plot of acoustic pressure and structural displacement can be done in the results module of *OpenPulse*. For example, a node at the left largest vertical tube (node 563) is analyzed in Fig. 9.

## 7. CONCLUSION

In this work, the authors presented physical and numeric details of the implementation of an open source software - the *OpenPulse* - with the objective of analyzing acoustically induced vibration caused in pipeline systems by low-frequency internal pulsation. The related project is in an early stage, but the first results present coherent significance, which can be validated with other commercial FEM codes (using 3D FEM acoustic analysis and 3D beam structures). The authors hope to publish a future work presenting different possibilities of using *OpenPulse* in more realistic examples, considering more piping elements (valves, chambers, etc) and comparing them with experimental results.

## 8. ACKNOWLEDGMENTS

The authors are grateful to Andre Fernandes, Lucas Kulakauskas and Diego Tuozzo.

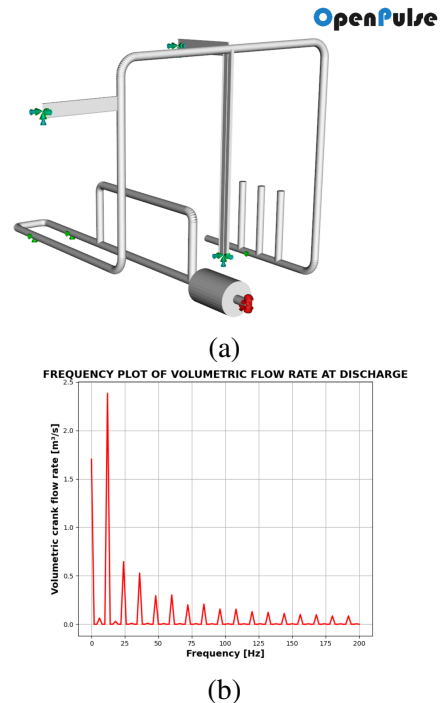


**Figure 6.** (a) Simple example of a piping system supported by “I” type beams. In red: discharge of a reciprocating compressor. In green: displacement constraints. (b) Frequency plot of volumetric flow rate at the discharge of a compressor.

## 9. REFERENCES

- [1] S. Kaneko, T. Nakamura, F. Inada, M. Kato, K. Ishihara, T. Nishihara, and M. A. Langthjem, eds., *Flow-induced Vibrations*. Oxford: Academic Press, second edition ed., 2014.
- [2] O. Silva, D. Tuozzo, J. Vargas, L. Kulakauskas, A. Fernandes, J. Souza, A. Rocha, A. Lenzi, R. Timbó, C. Mendonça, and A. Brandão, “Numerical modelling of low-frequency acoustically induced vibration in gas pipeline systems,” in *Proc. 29th International Conference on Noise and Vibration engineering (ISMA2020) - At: Online - Virtual Platform*, 09 2020.
- [3] S. Li, B. W. Karney, and G. Liu, “Fsi research in pipeline systems – a review of the literature,” *Journal of Fluids and Structures*, vol. 57, pp. 277 – 297, 2015.
- [4] A. Coulon, R. Salanon, and L. Ancian, “Innovative numerical fatigue methodology for piping systems:

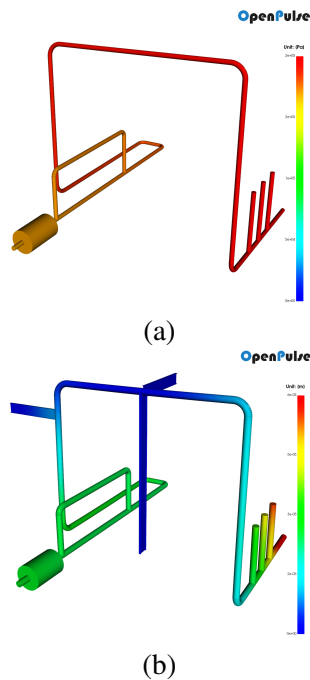


**Figure 7.** (a) Acoustic response and (b) structural response at 12 Hz. Colormap: amplitudes.

qualifying acoustic induced vibration in the oil & gas industry,” *Procedia Engineering*, vol. 213, pp. 762–775, 2018. 7th International Conference on Fatigue Design, Fatigue Design 2017, 29-30 November 2017, Senlis, France.

- [5] A. Craggs, “The application of the transfer matrix and matrix condensation methods with finite elements to duct acoustics,” *Journal of Sound and Vibration*, vol. 132, no. 3, pp. 393 – 402, 1989.
- [6] O. Silva, D. Tuozzo, J. Vargas, L. Kulakauskas, A. Fernandes, J. Souza, A. Rocha, A. Lenzi, R. Timbó, C. Mendonça, and A. Brandão, “Openpulse: Open source software for pulsation analysis of pipeline systems.” [%urlhttps://open-pulse.github.io/OpenPulse/](https://open-pulse.github.io/OpenPulse/), 2021.
- [7] J. Vargas, O. Silva, D. Tuozzo, L. Kulakauskas, A. Fernandes, J. Souza, A. Rocha, and A. Lenzi, “Openpulse: An open source software for pulsation analysis of pipeline systems,” in *Proc. of FIA 2022*, 2022.
- [8] F. Axisa and J. Antunes, “Chapter 4 plane acoustical waves in pipe systems,” in *Fluid-Structure Interaction*

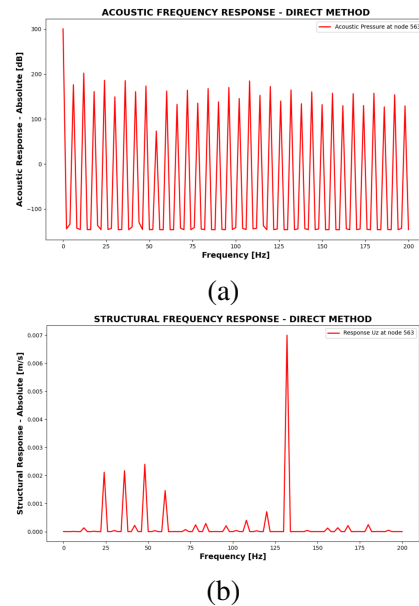


**Figure 8.** (a) Frequency plot of pressure amplitude and (b)  $x$ -velocity amplitude at node 563.

(F. Axisa and J. Antunes, eds.), vol. 3 of *Modelling of Mechanical Systems*, pp. 243 – 352, Butterworth-Heinemann, 2007.

- [9] A. Tesár and L. Fillo, *Transfer matrix method. Mathematics and its applications* (Kluwer Academic Publishers): East European series, Kluwer Academic Publishers, 1988.
- [10] “Fluid vibration in piping systems—a structural mechanics approach, i: Theory,” *Journal of Sound and Vibration*, vol. 133, no. 3, pp. 423 – 438, 1989.
- [11] T. Hughes, *The Finite Element Method: Linear Static and Dynamic Finite Element Analysis*. Dover Civil and Mechanical Engineering.
- [12] L. Andersen and S. R. K. Nielsen, *Elastic Beams in Three Dimensions*.
- [13] A. Boresi, K. Chong, and J. D. Lee, *Elasticity in Engineering Mechanics*. Wiley, 2010.